Article

Not peer-reviewed version

Stress-inducible SCAN Factors Suppress the Stress Response and Are Biomarkers for Enhanced Prognosis in Cancers

Takanori Eguchi *, Mona Sheta, Stuart K Calderwood

Posted Date: 25 January 2023

doi: 10.20944/preprints202301.0454.v1

Keywords: cell stress response; heat shock protein 90 (HSP90); SCAN domain-containing proteins (SCAND); MZF1; heat shock factors (HSF); co-expression correlation; Kaplan-Meyer analysis; cancer patients prognosis

Article

Stress-Inducible SCAN Factors Suppress the Stress Response and Are Biomarkers for Enhanced Prognosis in Cancers

Takanori Eguchi [1,*], Mona Sheta [1,2] and Stuart K. Calderwood [3]

[1] Department of Dental Pharmacology, Faculty of Medicine, Dentistry and Pharmaceutical Sciences, Okayama University, Okayama 700-8525, Japan; p9mw1s0r@s.okayama-u.ac.jp (M.S.)
[2] Department of Cancer Biology, National Cancer Institute, Cairo University, Cairo 11796, Egypt
[3] Department of Radiation Oncology, Beth Israel Deaconess Medical Center, Harvard Medical School, Boston, MA 02115, USA; scalderw@bidmc.harvard.edu
* Correspondence: eguchi@okayama-u.ac.jp; Tel.: +81 86 235 6661

Abstract: The cell stress response is an essential system present in every cell for responding and adapting to extracellular environmental stimulations. A major program for stress response is the heat shock factor (HSF)–heat shock protein (HSP) system that maintains proteostasis in cells and promotes cancer progression. However, less is known about how the cell stress response is regulated by alternative transcription factors. Here, we show that the SCAN domain-containing transcription factors (SCAN-TFs) are involved in repressing the stress response in cancer. SCAND1 and SCAND2 are SCAN-TFs that can hetero-oligomerize with SCAN-zinc finger transcription factors, such as MZF1(ZSCAN6), for accessing DNA and transcriptionally co-repressing target genes. We found that heat stress induced the expression of both SCAND1 and MZF1(ZSCAN6) bound to HSP90 gene promoter regions in prostate cancer cells. SCAND1 and MZF1 blocked the heat shock responsiveness of HSP90 in prostate cancer cells. Gene expression of SCAND2, SCAND1 and MZF1 was negatively correlated with HSP90 expression in patients-derived prostate adenocarcinoma. MZF1 and SCAND2 were more highly expressed in paired normal tissues than in tumor tissues in several cancer types. High expression of SCAND2, SCAND1 and MZF1 correlated with enhanced prognoses of pancreatic cancer and head and neck cancers. Additionally, high expression of SCAND2 was correlated with better prognoses of lung adenocarcinoma and sarcoma. In contrast, high expression of HSP90AA1 correlated with poorer prognoses in several cancer types. These data suggest that the stress-inducible SCAN-TFs can function as a feedback system, suppressing excessive stress response and inhibiting cancers.

Keywords: cell stress response; heat shock protein 90 (HSP90); SCAN domain-containing proteins (SCAND); MZF1; heat shock factors (HSF); co-expression correlation; Kaplan-Meier plot; cancer patients prognosis

1. Introduction

The cell stress response is an intrinsic system to all cells responding and adapting to environmental stimulations. One of the representative stress response systems is the heat shock factor (HSF)–heat shock protein (HSP) program that maintains proteostasis in cells [1–4] and promotes cancer progression [5–7]. The HSF-HSP system was originally found to be activated in response to heat shock stress (HSS) while subsequently shown to be induced by oxidative stress, heavy metals, toxins and bacterial infections [1]. Such proteotoxic stresses cause protein misfolding and thus activate the HSF-HSP system. The HSF-HSP system is often activated in cancer [8–10].

Heat shock protein 90 (HSP90) is a stress-inducible protein chaperone that assists protein folding and re-folding to give the clients functionality in the intracellular space. As HSP90 has several hundred protein substrates (called 'clients'), it is involved in many cellular processes beyond protein folding, which include DNA repair, development, the immune response and neurodegeneration [11–15]. Elevated expression of HSP90 has been observed in many cancer types and correlates with poor prognosis, increased metastatic potential and resistance to therapy [16–19]. Moreover, the HSP90

Preprints (www.preprints.org) | NOT PEER-REVIEWED | Posted: 25 January 2023 doi:10.20944/preprints202301.0454.v1

alpha and beta isoforms are often released with extracellular vesicles (EV), including exosomes, by cancer cells and can thus trigger cancer initiation and progression, as well as the polarization of tumor-associated macrophages to an immunosuppressive M2 subtype [6,17,20–22]. In addition, HSP90 is produced and released by immunocytes, such as macrophages, and plays a key role in antigen cross-presentation [14,15,23,24]. HSF1 is the master regulator of the protein quality control machinery in response to proteotoxic stress conditions [2,3,25] and enhances cancer progression [5,7]. Upon proteotoxic stress, HSF1 binds to heat shock elements (HSEs) in the promoter regions of HSP genes and other stress-inducible genes [2,3,25]. HSF1 drives oncogenesis in many ways beyond inducing the gene expression of chaperones [7,26–28], co-chaperones [6], and non-chaperone target genes [9]. However, less is known about how HSP90 genes are attenuated by alternative transcription factors.

The SCAN domain-containing transcription factors (SCAN-TF) contain the SREZBP-CTfin51-AW1-Number 18 cDNA (SCAN) domain, a leucine-rich oligomerization domain highly conserved among the SCAN-TF family (Figure S1). This family contains more than 50 members, most of which contain a zinc finger (ZF) domain: hence SCAN-ZF factors [29–33]. Myeloid zinc finger 1 (MZF1), also known as ZSCAN6 or ZNF42, is a prototypical SCAN-ZF that contains an N-terminal SCAN domain, a linker region, and a C-terminal DNA binding domain [34–36]. Many studies have identified MZF1 as an oncogenic transcription factor [34,37–40] and cancer stemness factor [41,42]. However, depending on the context, MZF1 can also function as a tumor suppressor [43–45]. While there are more than 50 types of SCAN-TFs, six zinc-fingerless SCAN domain-only proteins also exist [30,31]. SCAND1 and SCAND2 (also known as SCAND2P) are SCAN domain-only proteins and can hetero-oligomerize with other SCAN-ZFs, including MZF1, through inter-SCAN domain interactions to repress transcription [32,33,37,43,46]. Thus, hetero-oligomerization between SCAN domain-only molecules and SCAN-ZF molecules can transform their roles, forming a transcriptional repressor complex [32,33,37,43,46]. Indeed, SCAND1 represses the co-chaperone *CDC37* gene (encoding cell division control 37) by interacting with MZF1 and suppressing prostate cancer progression [37]. Moreover, SCAND1 and MZF1 are mutually inducible and form oligomers that can reverse epithelial-to-mesenchymal transition (EMT), tumor growth and migration by repressing EMT driver genes and mitogenic protein kinase (MAPK) genes [43]. High expression of MZF1 was correlated with poor prognoses in prostate cancer and kidney cancer, whereas SCAND1 and MZF1 expression correlate with better prognosis in pancreatic cancer and head and neck cancers stage III [43]. These suggest that MZF1 alone is oncogenic, whereas repressing complexes of SCAND1 and MZF1 is tumor suppressor, depending on the gene expression in cancer cases.

However, it has been unclear whether the SCAND factors and MZF1 are involved in proteotoxic stress response in cancer. Here, we show that the SCANDs and MZF1 are stress-inducible factors and can attenuate HSP90 gene expression in prostate cancer cells. We also show that high expression levels of these SCAN-TFs can be predictive biomarkers of better prognoses in several cancer types, indicating potential tumor suppressor roles.

2. Results

2.1. Heat shock stress induces SCAND1 and MZF1(ZSCAN6) gene expression in prostate cancer

To predict whether SCAND1 and MZF1 genes are transcriptionally regulated by HSFs and MZF1, we searched binding sequences of these TFs in promoter regions. Several binding sequences (BS) for HSF1 and HSF4 were found in the promoter regions of SCAND1 and MZF1 genes (Table 1). Moreover, dozens of MZF1-BSs were found in the promoter regions of SCAND1 and MZF1 genes.

Table 1. The numbers of binding sites for HSF1, HSF4 and MZF1 in the promoter regions of SCAND1 and MZF1 genes.

Gene promoter [1]	HSF1-BS	HSF4-BS	MZF1-BS	MZF1-BS var.2
SCAND1	7	9	5	15
MZF1	4	4	27	30

Preprints (www.preprints.org) | NOT PEER-REVIEWED | Posted: 25 January 2023 doi:10.20944/preprints202301.0454.v1

[1] Promoter regions from –5000 to +1000 were analyzed. Numbers of binding sequences with p-values > 0.01 were counted.

We then asked whether SCAND1 and MZF1 expressions were inducible by heat shock stress (HSS). Indeed, gene expression of both SCAND1 and MZF1 was induced by HSS in DU-145 prostate cancer cells (Figure 1A,B). SCAND1 and MZF1 at protein levels were also increased and became localized in nuclei (Figure 1C,D).

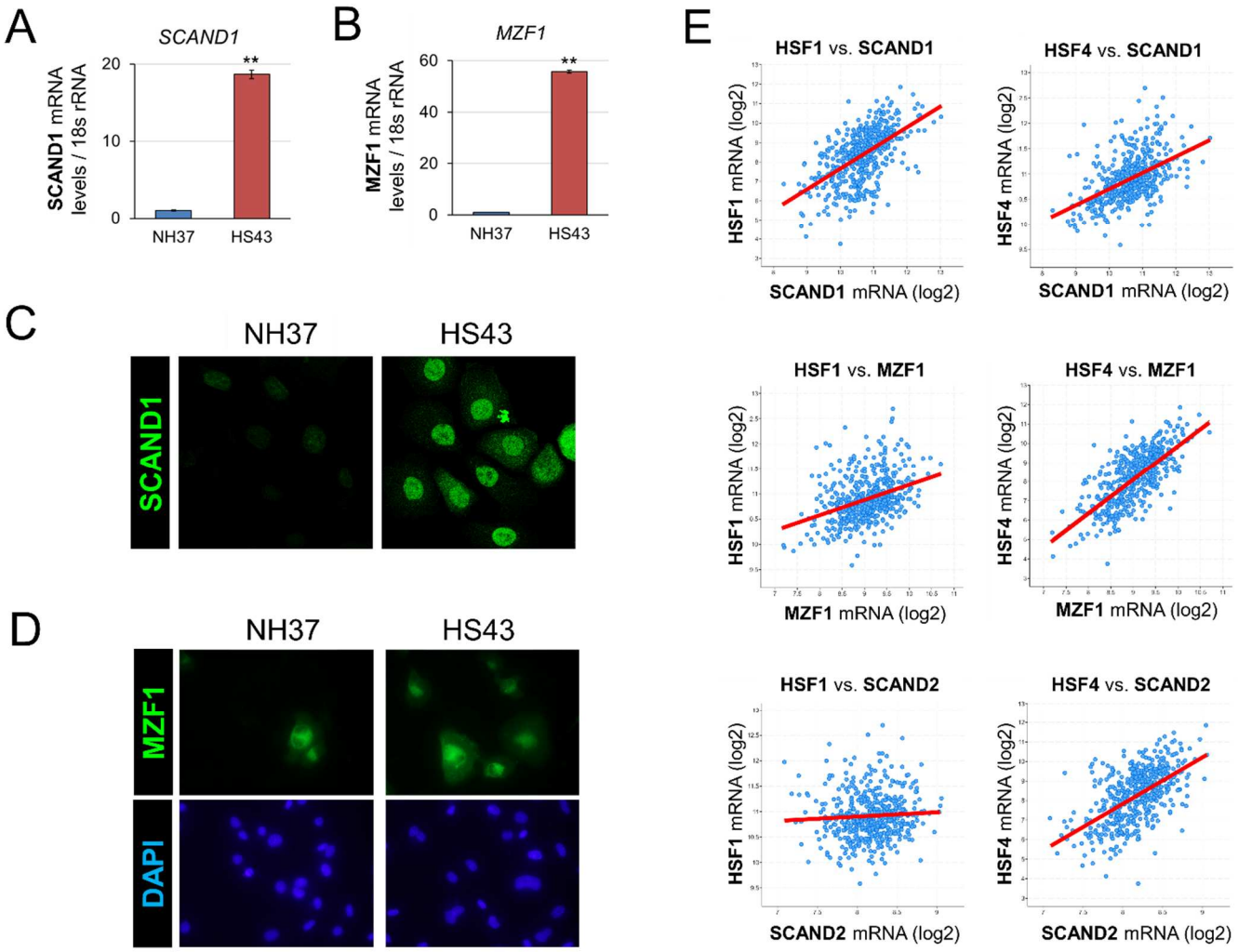

Figure 1. Heat shock stress induces SCAND1 and MZF1(ZSCAN6) in prostate cancer cells. (A,B) qRT-PCR analysis of SCAND1 (A) and MZF1 (B) mRNA expression upon HSS in DU-145 cells. NH37, non-heated at 37 °C. HS43, heat-shocked at 43°C for 30 min. **p < 0.01, n = 3 (C,D) immunocytochemistry of SCAND1 (C) and MZF1 (D) expressed with or witout heat shock. (E) Co-expression correlation between HSF1 or HSF4 vs. SCAND1, SCAND2, or MZF1 in patients-derived prostate adenocarcinoma.

We next examined whether the expression of SCAN-TFs (SCAND1, SCAND2, and MZF1) was correlated with HSF1 or HSF4 expression in prostate cancer specimens derived from patients. SCAND1 and MZF1 expression levels were correlated with the degree of expression of HSF1 and HSF4 (Figure 1E, Table 2). SCAND2 expression was correlated with the expression of HSF4 but not with HSF1.

These data suggested that SCAND1 and MZF1 are stress-inducible genes and that the stress inducibilities of SCAND1 and MZF1 could potentially be mediated by HSF1 and HSF4 in prostate cancer.

Preprints (www.preprints.org) | NOT PEER-REVIEWED | Posted: 25 January 2023 doi:10.20944/preprints202301.0454.v1

Table 2. Co-expression correlation between HSFs, MZF1 and SCANDs in prostate adenocarcinomas.

Gene	Correlated Gene	Spearman's Correlation [1]	p-Value	q-Value
HSF1 vs.	**MZF1**	**0.375**	9.52E-18	7.37E-17
HSF1 vs.	**SCAND1**	**0.518**	6.73E-35	2.92E-33
HSF1 vs.	**SCAND2**	0.0925	0.0412	0.0642
HSF4 vs.	**MZF1**	**0.705**	1.97E-74	3.03E-72
HSF4 vs.	**SCAND1**	**0.585**	3.99E-46	1.86E-44
HSF4 vs.	**SCAND2**	**0.55**	5.55E-40	1.89E-38

[1] Spearman's correlation > 0.3 were shown in bold.

2.2. Co-expression correlation of SCAN-TF genes in prostate cancer

We recently showed that MZF1 and SCAND1 gene expression could mutually induce each other's expression [43]. Moreover, several MZF1-BSs exist in the promoter regions of SCAND1 and MZF1 genes, as shown in Table 2. We analyzed co-expression correlations of MZF1, SCAND1, and SCAND2 genes in prostate cancer. In prostate adenocarcinoma specimens, the expression of MZF1 was positively correlated with both SCAND1 and SCAND2 expression (Figure 2 A-C; Table 3).

Therefore, these data suggested that MZF1 could induce SCAND1 and SCAND2 gene expression in prostate cancer.

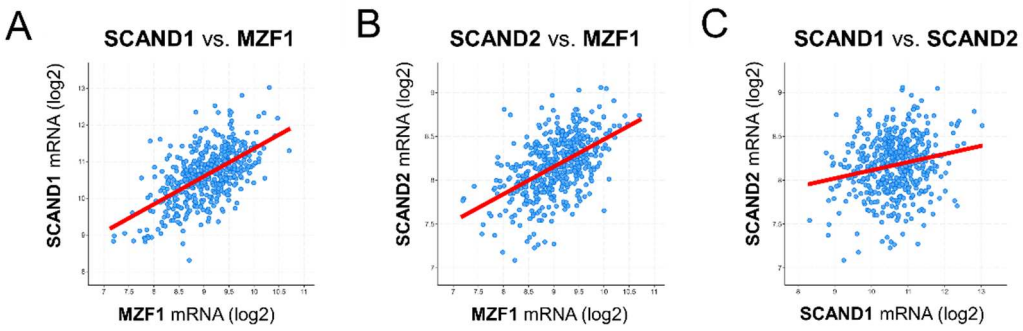

Figure 2. Co-expression correlation between MZF1, SCAND1, and SCAND2 in prostate cancer. (A) SCAND1 vs. MZF1, (B) SCAND2 vs. MZF1, (C) SCAND1 vs. SCAND2 in prostate adenocarcinoma specimens derived from patients.

Table 3. Co-expression correlation between HSFs, MZF1 and SCANDs in prostate adenocarcinomas.

Gene	Correlated Gene	Spearman's Correlation [1]	p-Value	q-Value
MZF1 vs.	**SCAND1**	**0.548**	1.27E-39	6.16E-38
MZF1 vs.	**SCAND2**	**0.524**	1.01E-35	3.95E-34
SCAND1 vs.	**SCAND2**	0.17	2.201E-4	4.160E-4

[1] Spearman's correlation > 0.3 were shown in bold.

2.3. Heat shock stress induces HSF1 and MZF1(ZSCAN6) binding to HSP90 genes

To ask whether *HSP90* genes were directly regulated by HSF1 and MZF1/ZSCAN6, we next analyzed promoter regions of *HSP90AA1* and *HSP90AB1* genes and performed ChIP-qPCR. The *HSP90AA1* promoter region (–5000 to +1000) contained 9 sites for HSF1 and 40 binding sites for MZF1. The *HSP90AB1* promoter region (–5000 to +1000) contained 8 binding sites for HSF1 and 50 binding sites for MZF1 (Table 4; Figure 3A, B). These data indicated that *HSP90* genes could be potential targets for the HSF1 and MZF1-SCAND complex.

Preprints (www.preprints.org) | NOT PEER-REVIEWED | Posted: 25 January 2023 doi:10.20944/preprints202301.0454.v1

Table 4. The numbers of binding sites for HSF1, HSF4 and MZF1 in the promoter regions of HSP90AA1 and HSP90AB1 genes.

Promoter	HSF1-BS	HSF4-BS	MZF1-BS	MZF1-BS var.2
HSP90AA1	9	12	22	18
HSP90AB1	8	8	22	28

[1] Promoter regions from –5000 to +1000 were analyzed. Numbers of binding sequences with p-values > 0.01 were counted.

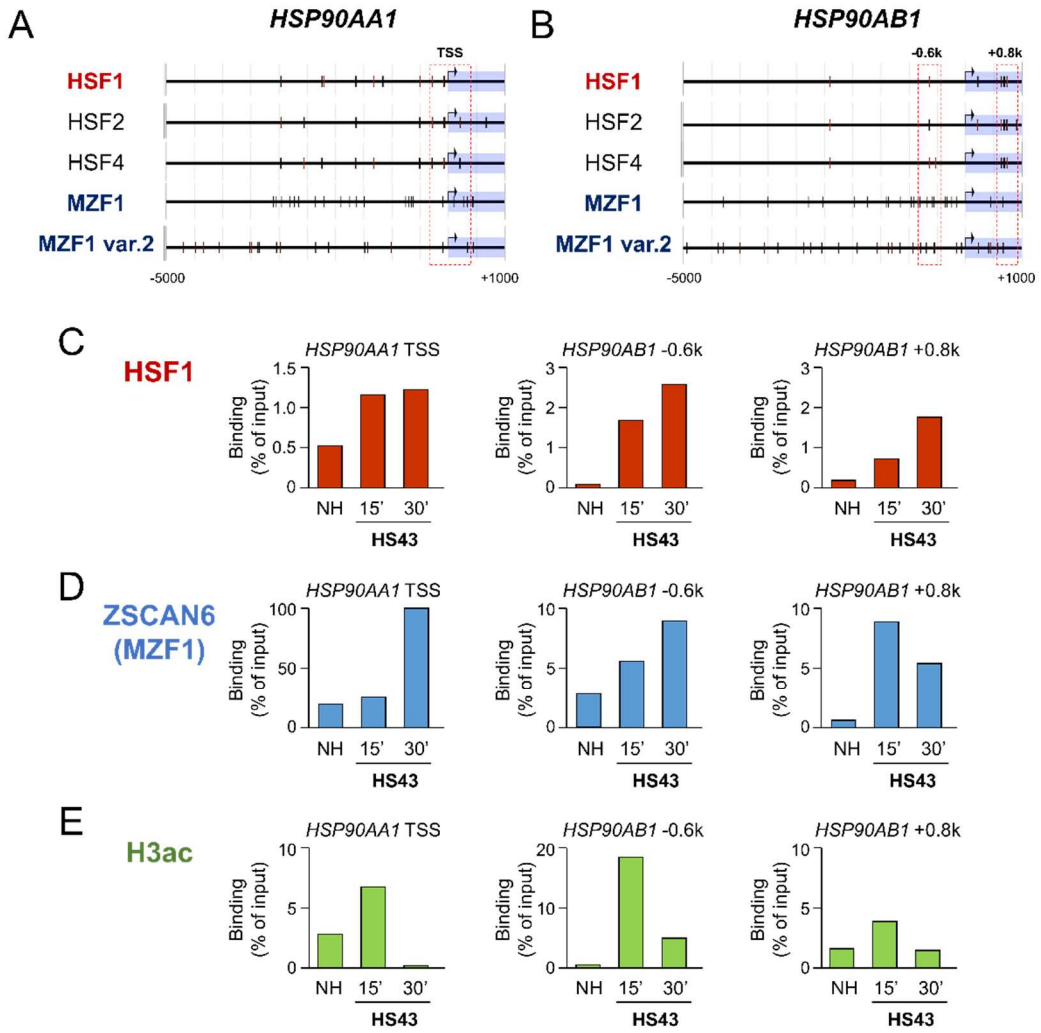

Figure 3. Heat shock stress induces HSF1 and MZF1(ZSCAN6) binding to HSP90 genes. (A, B) Promoter regions (–5000 to +1000) of *HSP90AA1* gene (A) and *HSP90AB1* gene mapped with binding sites of HSFs and MZF1(ZSCAN6). Black vertical bars indicate binding sites. Hatched boxes indicate regions analyzed by ChIP-qPCR. (C–) ChIP-qPCR assay. PC-3 cells were treated with heat shock at 43 ℃ (HS43) for 15 or 30 min or non-heated (NH), and chromatin was fixed. ChIP was performed using antibodies against HSF1 (C), MZF1/ZSCAN6 (D) and acetylated histone H3 (H3ac) (E) for qPCR of HSP90 genes.

We next performed ChIP-qPCR analysis to ask about the direct regulation of *HSP90* genes by HSF1 and MZF1(ZSCAN6). The binding of HSF1 to the *HSP90AA1* gene promoter region was increased in response to HSS in PC-3 prostate cancer cells (Figure 3C). MZF1(ZSCAN6) binding to the *HSP90AB1* gene promoter region was also increased in response to HSS (Figure 3D). Histone H3 acetylation, a marker of transcriptional activation, in the *HSP90AA1* gene promoter region was transiently increased in response to HSS in 15 min and then reduced in 30 min (Figure 3E).

Preprints (www.preprints.org) | NOT PEER-REVIEWED | Posted: 25 January 2023 doi:10.20944/preprints202301.0454.v1

These data suggested that HSF1 and MZF1 binding to the *HSP90* gene promoter regions could be transiently activating *HSP90* genes and repressing them later. Induction of SCAND expression upon HSS and its binding to MZF1 may function to turn off the transcription of *HSP90* genes in 30 min.

2.4. MZF1 and SCAND1 blocks the heat shock response of HSP90

We next examined whether MZF1 and SCAND1 could affect the heat shock response of the *HSP90AA1* gene. Indeed, HSP90AA1 mRNA expression was induced by HSS. However, MZF1 or SCAND1 overexpression blocked the HS response of HSP90AA1 gene expression (Figure 4A).

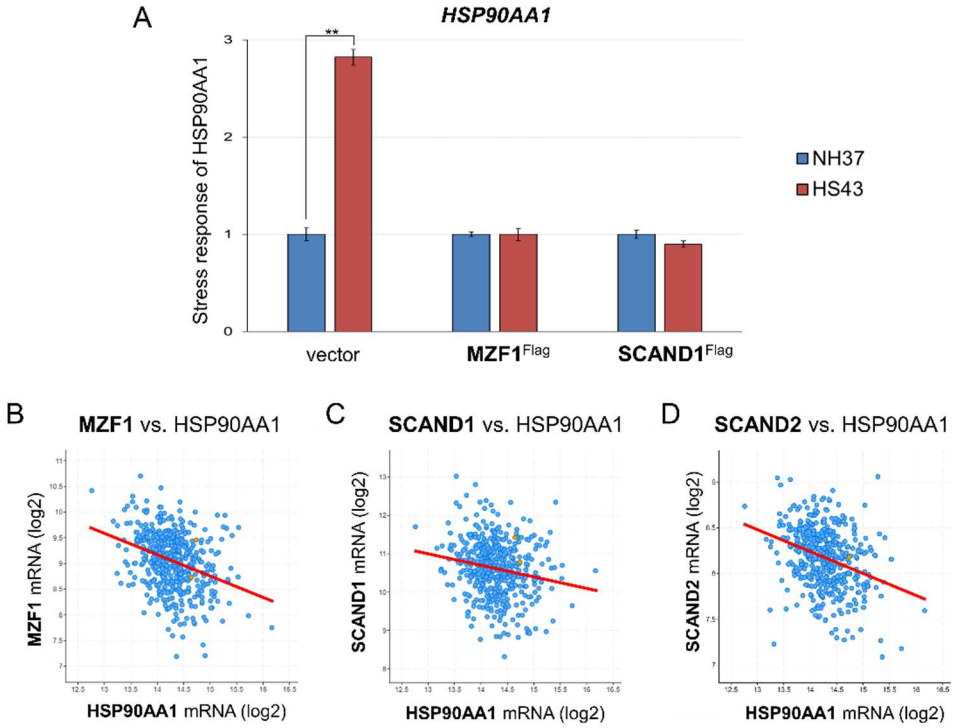

Figure 4. MZF1 and SCAND1 blocked the heat shock response of the *HSP90AA1* gene. (A) qRT-PCR for HSP90AA1 gene. Stable DU-145 cells transfected with pcDNA3.1 vector, pcDNA/MZF1-Flag and pCMV/SCAND1-Flag were treated with or without HSS for 30 min. **p<0.01, n=3. (B–E) Co-expression correlation between HSP90AA1 vs. MZF1(ZSCAN6) (B), SCAND1 (C) and SCAND2 (D) in prostate adenocarcinoma.

To ask whether HSP90AA1 is regulated by transcription factors, including SCAN-TFs and HSFs, we examined their co-expression correlation in prostate adenocarcinoma specimens. HSP90AA1 expression was negatively correlated with the expression of MZF1(ZSCAN6), SCAND1, SCAND2 and HSF4 in prostate adenocarcinoma specimens (Figure 4 B–D; Table 5). HSP90AA1 expression was not significantly correlated with the expression of HSF1, HSF2 and HSF5 in prostate adenocarcinoma specimens (Table 5).

We next examined whether other HSPs expression is correlated with these SCAN-TFs expression in addition to HSP90AA1. MZF1, SCAND1, and SCAND2 expressions are negatively correlated with gene expression of HSPA13, HSPA4, HSPA4L, and HSPH1 (Table 6, Table S1). These data suggested that SCAN-TFs co-repressed multiple HSP genes.

These data indicated that *HSP90AA1* gene expression was negatively regulated by MZF1(ZSCAN6), SCAND1, SCAND2 and HSF4 in prostate adenocarcinomas.

Preprints (www.preprints.org) | NOT PEER-REVIEWED | Posted: 25 January 2023 doi:10.20944/preprints202301.0454.v1

Table 5. The negative correlation of HSP90AA1 vs. MZF1, SCANDs and HSFs gene expression in prostate adenocarcinoma specimens.

Gene	Correlated Gene	Spearman's Correlation [1]	p-Value	q-Value
HSP90AA1 vs.	**MZF1**	**-0.321**	3.63E-13	3.35E-11
HSP90AA1 vs.	**SCAND2**	**-0.32**	4.34E-13	3.88E-11
HSP90AA1 vs.	**SCAND1**	**-0.188**	2.86E-05	1.71E-04
HSP90AA1 vs.	**HSF4**	**-0.241**	6.97E-08	9.73E-07
HSP90AA1 vs.	HSF1	-0.045	3.21E-01	4.38E-01
HSP90AA1 vs.	HSF2	-0.0164	7.17E-01	7.94E-01
HSP90AA1 vs.	HSF5	-0.00297	0.948	0.963

[1] Spearman's correlation < 0.15 were shown in bold.

Table 6. The negative correlation of HSPs vs. MZF1, SCAND1, and SCAND2 gene expression in prostate adenocarcinoma specimens.

	vs. MZF1		vs. SCAND1		vs. SCAND2	
Correlated Gene	Spearman's Correlation[1]	p-Value[2]	Spearman's Correlation	p-Value	Spearman's Correlation	p-Value
HSPA13	**-0.448**	**1.75E-25**	**-0.572**	**7.79E-44**	**-0.357**	**4.18E-16**
HSPA4	**-0.358**	**3.41E-16**	**-0.303**	**7.97E-12**	**-0.394**	**1.52E-19**
HSPA4L	**-0.326**	**1.58E-13**	**-0.411**	**2.66E-21**	-0.0341	0.452
HSP90AA1	**-0.321**	**3.63E-13**	-0.188	2.86E-05	**-0.32**	**4.34E-13**
HSPH1	**-0.300**	**1.42E-11**	-0.191	2.20E-05	**-0.312**	**1.67E-12**

[1] Spearman's correlation < 0.25 were shown in bold. [2] p-Values < 1E–10 were shown in bold.

2.5. Reduced expression of SCAND2 and MZF1 coincide with the increased HSP90 expression in tumor tissues compared to normal tissues

We next hypothesized that the repressing factors SCAND2 and MZF1 were reduced in tumor tissues while HSP90 gene expression was increased in tumor tissues. SCAND2 and MZF1(ZSCAN6) expression were lower in prostate adenocarcinoma (PRAD), breast invasive carcinoma (BRCA), colon adenocarcinoma (COAD), rectum adenocarcinoma (READ), skin cutaneous melanoma (SKCM), testicular germ cell tumors (TGCT) and uterine carcinosarcoma (UCS) while HSP90AA1 and HSP90AB1 expression were higher in these cancer types as compared to paired normal tissues (Figure 5, Figure S2). Exceptionally, SCAND2 and MZF1(ZSCAN6) expression were higher in acute myeloid leukemia (LAML), while HSP90AA1 and HSP90AB1 expression were lower, as compared to paired normal tissues.

These data suggested that reduced expression of SCAND2 and MZF1 could result in the elevated expression of HSP90 genes in tumor tissues in many cancer types.

Preprints (www.preprints.org) | NOT PEER-REVIEWED | Posted: 25 January 2023 doi:10.20944/preprints202301.0454.v1

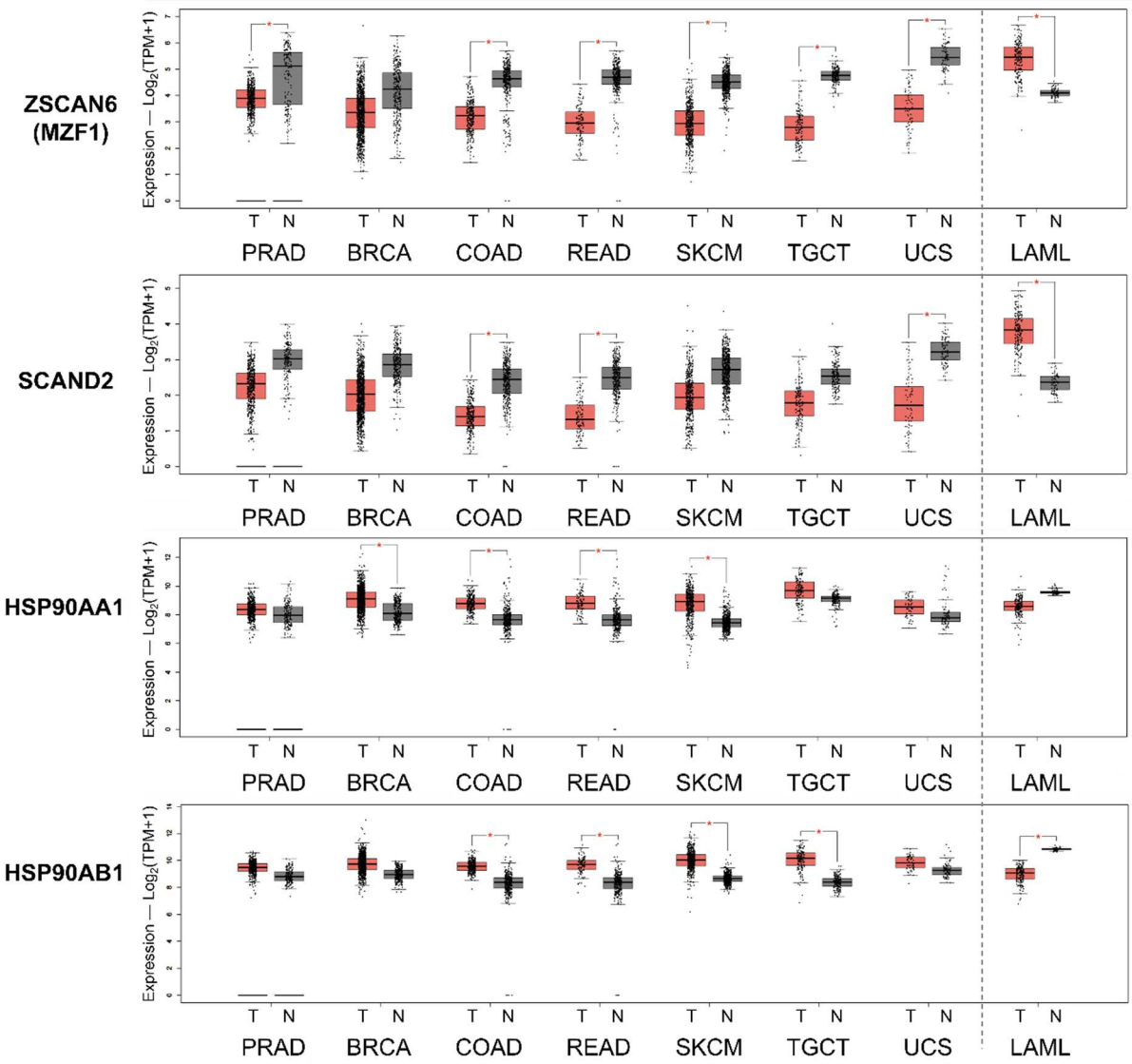

Figure 5. Gene expression levels of ZSCAN6(MZF1), SCAND2, and HSP90 in various tumor types vs. paired normal tissues. Red box, tumor tissues (T). Gray box, normal tissues (N). Prostate adenocarcinoma (PRAD), breast invasive carcinoma (BRCA), colon adenocarcinoma (COAD), rectum adenocarcinoma (READ), skin cutaneous melanoma (SKCM), testicular germ cell tumors (TGCT), uterine carcinosarcoma (UCS), and acute myelo1id leukemia (LAML).

2.6. SCANDs and MZF1(ZSACAN6) expression were correlated with enhanced prognoses whereas HSP90 expression is correlated with poor prognoses in cancers.

We next hypothesized that the repressive transcription factors SCAND1, SCAND2 and MZF1(ZSCAN6) would contribute to enhanced prognosis in cancer patients, whereas high expression of HSP90 genes would likely be involved in a poorer prognosis. High expression of SCAND1, SCAND2 and MZF1 was significantly correlated with enhanced prognosis of patients suffering from pancreatic ductal adenocarcinoma (DAC) (Figure 6 A, B, C; Table 7). High expression of HSP90AA1 and HSP90AB1 (associated with a low MZF1 expression scenario) was significantly correlated with poorer prognosis of patients suffering from pancreatic cancer (Figure 6 D, E, F).

Similarly, high expression of SCAND2, SCAND1 and MZF1 was significantly correlated with enhanced prognosis of patients suffering from head and neck squamous cell carcinoma (SCC) stage III (Figure 7 A, B, C), whereas high expression of HSP90AA1 and HSP90AB1 was significantly correlated with poorer prognosis of patients suffering from head and neck SCC stage III (Figure 7 D, E, F).

Preprints (www.preprints.org) | NOT PEER-REVIEWED | Posted: 25 January 2023 doi:10.20944/preprints202301.0454.v1

Table 7. SCAND1, SCAND2 and MZF1 expression correlate with enhanced prognoses in cancer.

Cancer type	Log-rank P		
	SCAND2	SCAND1	MZF1
Pancreatic cancer	0.00018***	0.0041**	0.0009**
Head & Neck SCC stage III	0.045*	0.024*	0.018*
Lung adenocarcinoma	0.00032***	0.32	0.21
Sarcoma	0.0096**	0.11	0.14
Cervical SCC	0.015*	0.34	0.21

*p<0.05, **p<0.05, ***p<0.0001.

High expression of SCAND2 and MZF1 was significantly correlated with enhanced prognosis of patients suffering from lung adenocarcinoma (Figure S3 A, B, C). Consistent with this, high expression of HSP90AA1 and HSP90AB1 was significantly correlated with poorer prognosis of patients suffering from lung adenocarcinoma (Figure S3 D, E, F).

Moreover, high expression of SCAND2 was correlated with enhanced prognoses in sarcoma and cervical SCC (Table 7).

These data suggested that high expression of SCAND2, SCAND1 and MZF1 were superior prognostic markers in several cancer types, including pancreatic cancer, head and neck cancers, lung adenocarcinoma, sarcoma and cervical cancer.

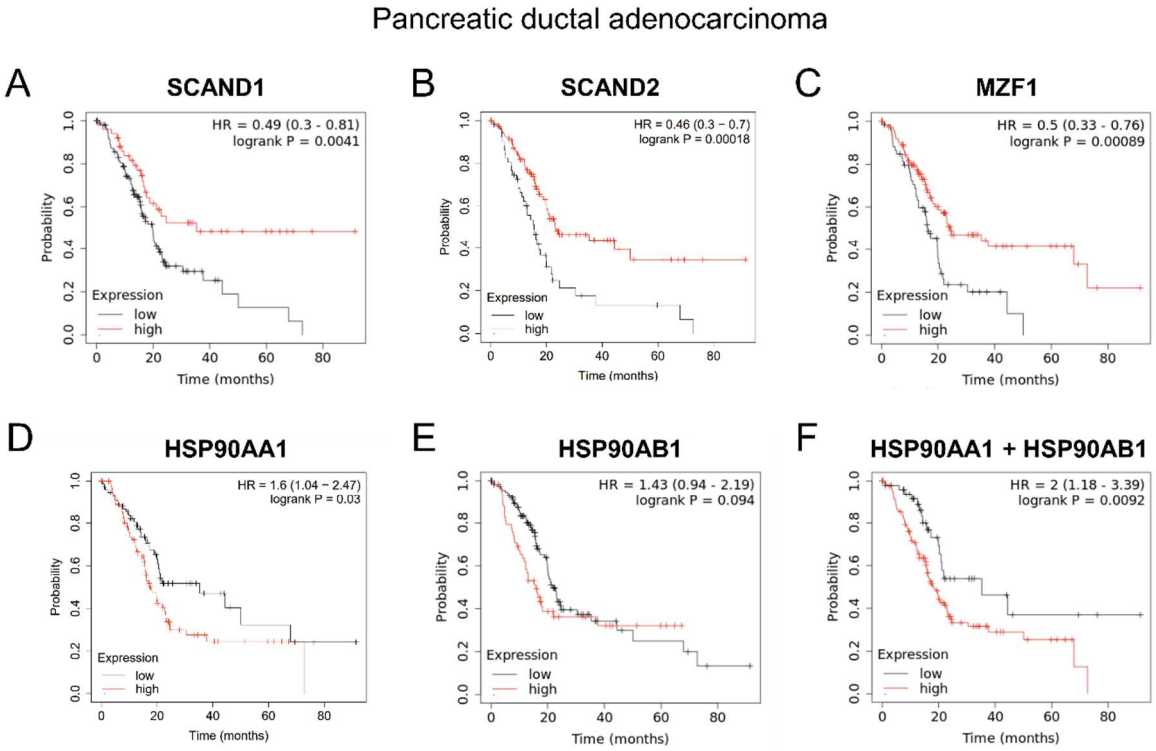

Figure 6. Kaplan-Meier plots showing prognostic values of SCANDs, MZF1, and HSP90 gene expression in pancreatic cancer. SCANDs and MZF1 expression are correlated with better prognoses whereas HSP90 expression is correlated with poor prognosis of pancreatic DAC.

Preprints (www.preprints.org) | NOT PEER-REVIEWED | Posted: 25 January 2023 doi:10.20944/preprints202301.0454.v1

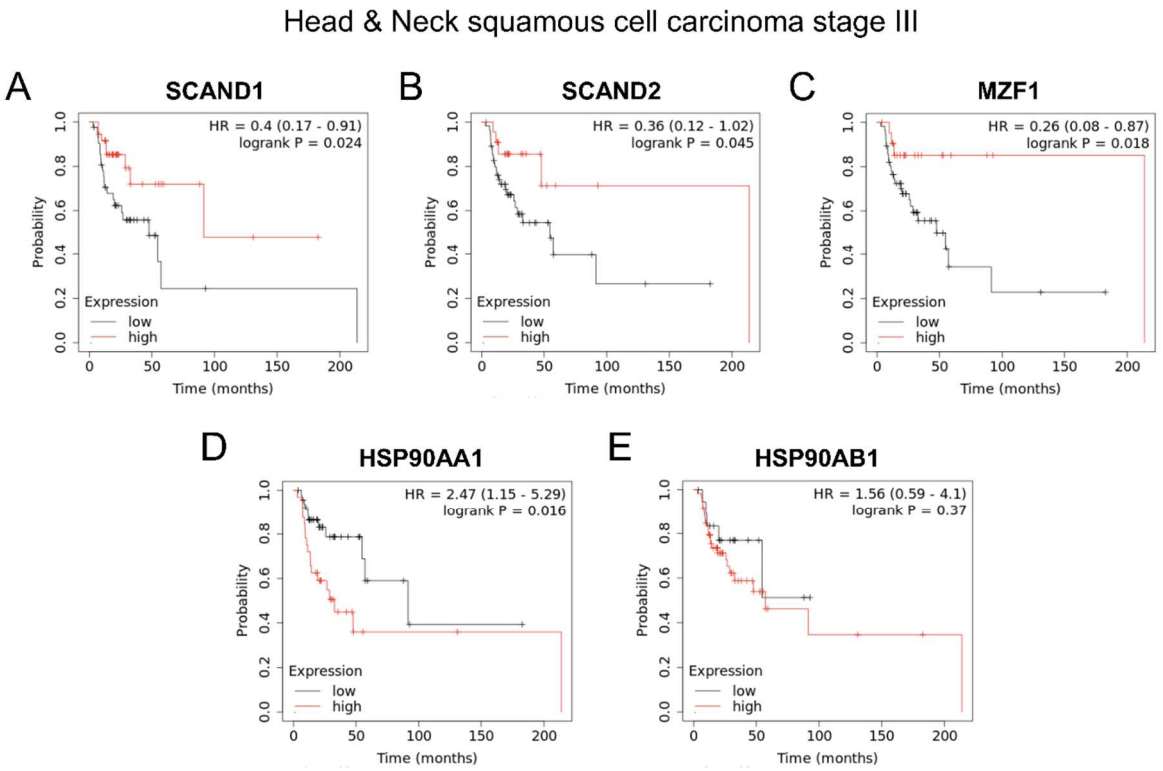

Figure 7. Kaplan-Meier plots showing prognostic values of SCANDs, MZF1, and HSP90 gene expression in head and neck cancers. SCANDs and MZF1 expression are correlated with better prognosis, whereas HSP90 expression is correlated with poor prognosis of head and neck SCC.

3. Discussion

We have shown that the cell stress-inducible SCAND1 and MZF1 genes repress the stress response of the HSF-HSP system (Figure 1–4). SCAND1 and MZF1/ZSCAN6 are heat-inducible and could form repressing complexes on HSP90 genes (Figure 8) [37,43]. These findings were consistent with the data from clinical tumor specimens. SCAND2 and MZF1 were expressed at higher levels in normal tissues than in paired tumor tissues (Figure 5). In contrast, HSP90 was expressed at higher levels in tumor tissues than paired normal tissues in many cancer types (Figure 5), suggesting that SCAND2/MZF1 hetero-oligomers could inhibit excess stress response of HSP90 expression in normal tissues, whereas loss of these SCAN-TF expressions could result in the gain of HSP90 in tumor tissues. We showed that high expressions of SCAN-TFs (SCAND1, SCAND2, and MZF1) were predictive biomarkers of enhanced prognoses for patients suffering from pancreatic cancer and head and neck cancers (Figure 6,7). Moreover, high expression of SCAND2 was a predictive biomarker of enhanced prognoses for patients suffering from lung adenocarcinoma, sarcoma, and cervical cancer (Table 7). These data indicate that SCAND/MZF1 repressing complexes are potentially tumor suppressing, contributing to better prognoses of patients suffering from several cancer types.

Our data, for the first time, indicate that SCAND2 is a novel biomarker of better prognoses in patients suffering from cancers (Table 6). Only one group has previously reported the existence of the *SCAND2* gene [47]. Moreover, SCAND2 has been registered as *SCAND2P*, a pseudogene. However, gene expression data of SCAND2 (or SCAND2P) were found in many databases. Of note, the protein structure of SCAND2 found in Phosphosite plus is more conserved with the N-terminal region of MZF1(ZSCAN6) than SCAND1 (Figure S1). Consistently, SCAND2 and MZF1 mRNA were each expressed in normal tissue at higher levels than tumor tissues (Figure 5), whereas SCAND1 expression did not show this pattern. Therefore, SCAND2 may form stabler hetero-oligomers with MZF1(ZSCAN6) than SCAND1 to repress oncogenic gene expression in tumors. However, further functional analysis of SCAND2 is required for this novel gene.

Preprints (www.preprints.org) | NOT PEER-REVIEWED | Posted: 25 January 2023 doi:10.20944/preprints202301.0454.v1

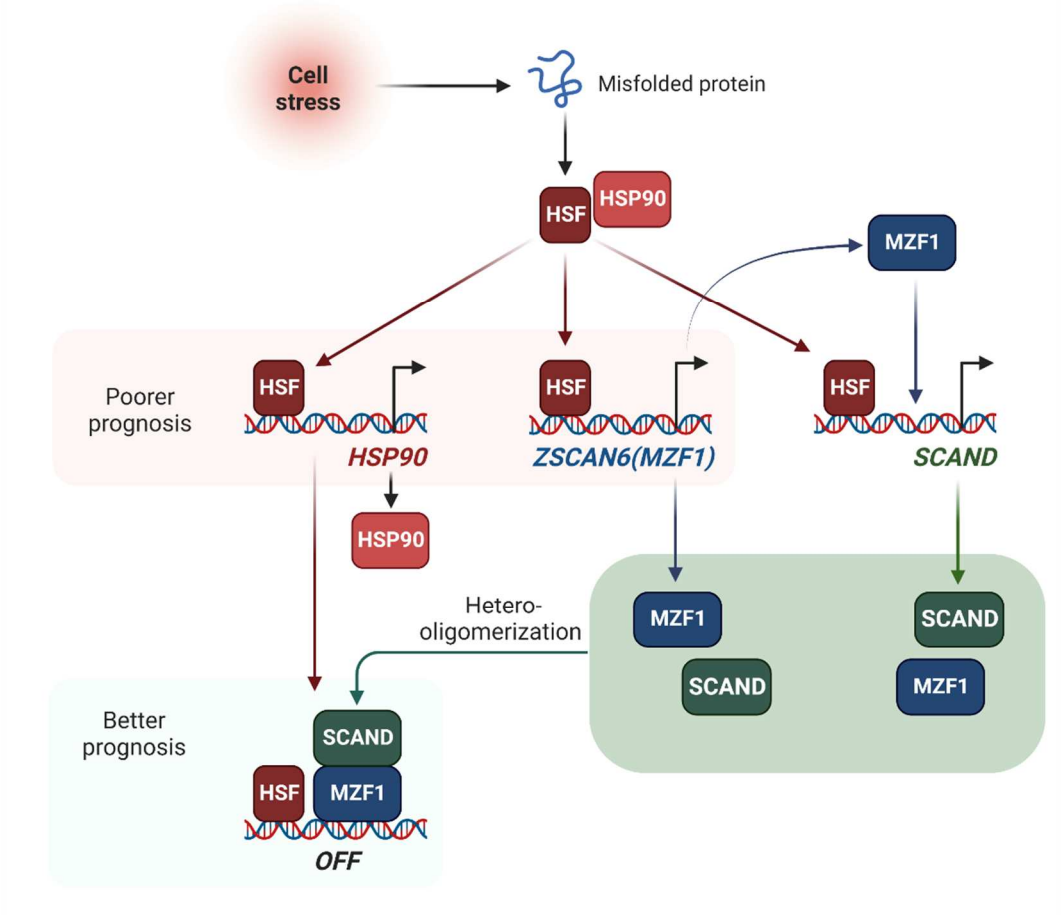

Figure 8. Stress-inducible SCAN transcription factors SCAND and MZF1 repress *HSP90* gene expression. Cell stress activates HSF1 leading to binding to HSEs in the promoter regions of *HSP90* genes (*HSP90AA1* and *HSP90AB1*), *ZSCAN6(MZF1)* gene and *SCAND* genes (*SCAND1* and *SCAND2*). MZF1 induces SCAND1 expression. Hetero-oligomers of MZF1 and SCAND bind to and repress *HSP90* genes.

Our data also suggest that SCAND2 can be a novel potent tumor suppressor. SCAND1 and MZF1 expression were positively correlated with HSF1 expression, whereas SCAND2 expression was not correlated with HSF1 expression, suggesting that SCAND2 is not heat stress-inducible (Figure 1). However, HSF4 expression was positively correlated with the expression of SCAND1, SCAND2 and MZF1, suggesting that HSF4 could induce these SCAN-TF gene expressions. HSF4 lacks a leucine zipper 4 (LZ4) domain, resulting in its constitutive trimerization and DNA-binding activity [48]. Several HSF4-BSs were found in the promoter regions of SCAND1 and MZF1 genes (Table 1). Thus, the expression of HSF4 could result in the constitutive expression of SCAND2, SCAND1, and MZF1 without cell stress. HSF4 is oncogenic in colorectal cancer, hepatocellular carcinoma, and lymphoma [49–51]. However, HSF-dependent expression of SCAN-TFs may reduce oncogenic gene expression in tumors.

Our data also suggested that the stress-inducible SCAND-MZF1 complex represses the HSP90AA1 gene while repressing other HSPs and many more stress-responsive genes (Table S1, Table 6). We have recently shown SCAND1 and MZF1 expression to be negatively correlated with EMT driver genes, including ZEB1, CTNNB1 and TGFBR1/2/3, and mitogenic genes encoding kinases in the MEKK-MEK-ERK signaling pathway [43]. Moreover, SCAN-only family genes and MZF1 expression were negatively correlated with the expression of NF-κB signaling molecules and PI3K-AKT signaling molecules (Data not shown). Thus, we have shown that EMT, some oncogenic signaling pathways and the HSF-HSP gene expression system are all key targets of the repression complex SCAND-MZF1.

Preprints (www.preprints.org) | NOT PEER-REVIEWED | Posted: 25 January 2023 doi:10.20944/preprints202301.0454.v1

Our data also suggested that tumors' stress levels differed among clinical cases (Figures 4, 5). Tumor cells are characteristically exposed to various stresses from the microenvironment, such as immune/inflammatory stress [19], therapeutics [18], hypoxia [22,52–55], acidification [56,57], hyperthermia [58,59] or heat stress [4,6,19,25,28], endoplasmic reticulum stress [60], nuclear envelope stress [61,62], replication stress [63], oxidative stress [64], mechanical stress, osmotic stress, genotoxic (DNA damage) [65,66] and proteotoxic stress [1,2,4,67]. Therefore, it might be difficult to determine the types and levels of stresses in each tumor. However, there were strong correlations between the expression of SCAN-TFs and HSP90AA1 in clinical tumor specimens (Figure 4–7). These clinical data support that the SCAN-TFs complex represses excessive expression of HSP genes and suppresses tumors.

In conclusion, we have demonstrated that the cell stress-inducible SCAND and MZF1 repress the stress response in cancer. MZF1 and SCAND1 are mutually inducible and can form a repressive complex on the HSP90 gene promoters. Moreover, elevated levels of SCAND are novel potential markers of better prognoses in several cancer types, including pancreatic cancer, head and neck cancers, lung adenocarcinoma, sarcoma, and cervical cancer. This effect may ensue from the findings that the SCAND-MZF1 repressive system is important for preventing cancer-related gene expression physiologically while playing a key role in tumor suppression.

4. Materials and Methods

4.1. Cell culture

Prostate cancer cell lines DU-145 and PC-3 were provided by ATCC and cultured in DMEM and RPMI medium, respectively, with 10% FBS.

4.2. Promoter analysis

Promoter analysis was performed using the Eukaryotic Promoter Database (EPD) https://epd.epfl.ch//index.php [68]. Binding motifs for HSF1, HSF2, HSF4, MZF1 and MZF1 var.2 were used from the Library of Transcription Factor Motifs (JASPAR CORE 2018 vertebrates). DNA sequences of 5′-flanking regions and gene bodies (–5000 to +1000 bp relative to TSS) of *SCAND1, MZF1, HSP90AA1* and *HSP90AB1* genes in human (Homo sapiens) were analyzed with a cut-off (p-value) of 0.001.

4.3. Heat shock stress

For HSS, the medium was replaced with an incubated medium at 43 or 37 °C and then put in a water bath at 43 or 37 °C, as described previously [6,28].

4.4. Plasmids and transfection

We used pcDNA3.1 (as a control), pcDNA3/MZF1^{Flag} and pCMV6/SCAND1$^{myc\text{-}Flag}$ (variant 1, purchased from OriGene, accession number NM_016558) as previously described [37]. DU-145 cells were transfected with these plasmids using Lipofectamine 2000 (Thermo Fisher Scientific) and cultured with 0.8 μg/ml of geneticin for 2 weeks to establish stable clones as described previously [43].

4.5. Immunocytochemistry and CLSM

Immunocytochemistry and confocal laser scanning microscopy (CLSM) were performed as previously described [69,70]. Cells were cultured on 12-mm round coverslips coated with poly-D-Lysine/Laminin (BD Bioscience, Franklin Lakes, NJ). Cells were fixed with 4% paraformaldehyde, then permeabilized with 0.1% Triton X-100 for 10 min. Cells were incubated in a blocking buffer containing 3% normal goat serum in PBS for 30 min, incubated with primary antibodies at 4℃ overnight and then secondary antibodies at RT for 1 hour in the blocking buffer. Cells were washed thrice with PBS for 5 min between the steps. Cells were mounted within ProLong Gold Antifade

Preprints (www.preprints.org) | NOT PEER-REVIEWED | Posted: 25 January 2023 doi:10.20944/preprints202301.0454.v1

Mountant (Thermo Fisher Scientific). Fluorescence images were acquired using Axio Vision CLSM (Zeiss, Oberkochen, Germany) with a camera AxioCam MR3 (Zeiss) and a filter set for DAPI, GFP, Cy3.5 (excitation wavelength: 580 nm) and Cy5 (excitation wavelength: 650 nm). We used anti-SCAND1 (ab64828, Abcam, Rb) antibody and anti-rabbit IgG conjugated with Alexa Fluor 488 (Thermo Fisher Scientific).

4.6. qRT-PCR

qRT-PCR was performed as previously described [37,70]. Total RNA was prepared with *DNase* I treatment using RNeasy columns (Qiagen, Hilden, Germany). cDNA was synthesized using QuantiTect kit (Qiagen), a mixture of oligo dT and random primers, then diluted 5 fold in 10 mM Tris-Cl and 0.1 mM EDTA buffer. A step dilution of the cDNA pool was prepared as a standard for relative expression. cDNA (4–10 µl), 0.25 µM of each primer and 10 µl SYBR green 2x Master Mix (Applied Biosystems, Waltham, MA) were mixed and filled up to a 20 µl of a reaction mixture. We designed and used primer pairs (Table 6).

Table 6. Primer sequences for qRT-PCR.

Primer name	Sequences (5′ to 3′)
SCAND1 h F#1	CGC AGA GAA GCC AGA GAC TT
SCAND1 h R#10	TCA GCA CTG CGT CTG CAC C
MZF1 h F785	TGC AGG TGA AAG AGG AGT CA
MZF1 h R939	AGT CTT GCT GTG GGG AAA GA
HSP90AA1 h F1227	GAG CAG TAC GCT TGG GAG TC
HSP90AA1 h R1227	TCC ACG ACC CAT AGG TTC AC
18s rRNA h F1245	GAC TCA ACA CGG GAA ACC TC
18s rRNA h R1364	AGA CAA ATC GCT CCA CCA AC

4.7. ChIP

PC-3 cells were cultured in 150-mm dishes and heat-shocked for 0, 15, and 30 min. ChIP was performed using a magnetic beads-based ChIP assay kit (Merck/Millipore, Kenilworth, NJ). Briefly, endogenous proteins/DNA were cross-linked within 5% formaldehyde. Cells were collected by cell scrapers and centrifugation at 600 × *g* for 5 min and resuspended in a ChIP buffer (10 mM Tris, pH 8.0, 200 mM KCl, 1 mM $CaCl_2$, 0.5% NP-40) containing protease phosphatase inhibitor cocktail (Sigma). Cells were treated with 3 cycles of sonication on ice with a sonicator. One cycle was a 5-sec sonication with a 15-sec interval at 100% power. OD260 was measured to obtain brief reference DNA concentrations. Sonicated cells containing 10–20 µg DNA or 1 x 10^6 cells were treated with *MNase* at a final concentration of 100 unit/ml in 500 µl of ChIP buffer and incubated at 37°C for 40 min and then centrifuged at 15,000 × *g* at 4°C for 10 min. Sheared chromatin DNA in the supernatants was analyzed in 2% agarose gel electrophoresis. For antibody-beads preparation, 20 µl M280 sheep anti-rabbit IgG magnetic beads (Thermo Fisher Scientific) with 2 µg antibodies against MZF1 (C10502, Assay Biotechnology, Fremont, CA), HSF1 (#4356, Cell Signaling Technology) or acetylated histone H3 (06-599, Millipore) were solved in 500 µl ChIP buffer and then rotated for 3 hours or overnight. DNA purification and qPCR were performed as above-described. Primer sequences for ChIP-qPCR were listed (Table 7).

Table 7. Primer sequences for ChIP-qPCR.

Primer name	Sequences (5′ to 3′)
HSP90AA1 h -100F	GGCTGGGGAGGGTTCTTC
HSP90AA1 h +200R	GAGGCCTCCGGAATAGAAAG
HSP90AB1 h -800F	CCTGAGGATTGGGCTGGTA
HSP90AB1 h -430R	CATCTGCCCTACACATCTCG

 doi:10.20944/preprints202301.0454.v1

HSP90AB1 h +600F	GTCTCCAGCACCCGATACTC
HSP90AB1 h +900R	GAACAGGACCAAACCCAAGA

4.8. Co-expression analysis

A data set of prostate adenocarcinomas (Project ID: TCGA-PRAD, dbGaP study accession: phs000178, PanCancer Atlas; 494 patients/samples) was analyzed with Spearman's rank correlation coefficient of co-expression using cBioPortal [71,72].

4.9. Gene expression profiling of tumors vs. paired normal tissues

The gene expression profile across tumor samples and paired normal tissues (bar plot and box plot) were analyzed using GEPIA2 (http://gepia2.cancer-pku.cn) [73]. The P-value cutoff was 0.01 as default. Graphs were expressed as a log scale.

4.10. Kaplan-Meier analysis

Kaplan-Meier plotting from RNA-seq data was performed using KM plotter (https://kmplot.com/analysis) [74]. We analyzed the overall survival of patients suffering from pancreatic ductal adenocarcinoma (DAC) n=177, head and neck squamous cell carcinoma (SCC) stage III (n=78), lung adenocarcinoma (n=504), sarcoma (n=259) and cervical SCC (n=304) using KM plotter with auto-select best cutoff.

4.11. Statistics

Values of two groups were compared with an unpaired Student's *t*-test. $P < 0.05$ was considered to indicate statistical significance. Data were expressed as Mean ± SD unless otherwise specified.

Supplementary Materials: The following supporting information can be downloaded at: www.mdpi.com/xxx/s1, Figure S1: Protein structures of MZF1(ZSCAN6), SCAND1, and SCAND2; Figure S2: Gene expression profiling of SCAND2, ZSCAN6(MZF1), and HSP90 genes in various tumor types vs. paired normal tissues; Figure S3: Kaplan-Meier analysis of SCAN-TFs and HSP90 expression in lung adenocarcinoma. SCAND2; Table S1, co-expression correlation of SCAN-TF genes vs. HSPs in prostate adenocarcinoma specimens.

Author Contributions: T.E. conceived and conceptualized the study. S.K.C. and T.E. provided resources. T.E. provided methodology. T.E. and S.K.C. acquired funding. T.E. and M.S. performed experiments and formal analysis. T.E. and M.S. analyzed clinical data. T.E. interpreted the data. T.E. wrote a draft of the manuscript. S.K.C. reviewed and edited the manuscript.

Funding: T.E. was supported by JSPS Kakenhi grants 22F22409-TE/MS, 22H03511-HO, 21H03119-TY, 21K08902-HY, 20K09904-CS, 20H03888-HN, 20K20611-MT, and Wesco Scientific Promotion Foundation. M.S. was supported by Japan Society for the Promotion of Science International Research Fellowship in Japan. S.K.C. was supported by NIH grants R01CA176326 and CA176326-05.

Institutional Review Board Statement: Not applicable.

Informed Consent Statement: Not applicable.

Data Availability Statement: TCGA PanCancer Atlas and co-expression data are available in cBioPortal (cbioportal.org/). Gene expression profiling data were available in GEPIA2 (gepia2.cancer-pku.cn). Kaplan-Meier datasets are available in KM plotter (kmplot.com).

Acknowledgments: We appreciate Kuniaki Okamoto, Kisho Ono, Thomas Prince, and Kunihiro Yoshida for useful discussion, technical assistance, and lab management. The last figure was generated using BioRender.

Conflicts of interest: The authors declare no conflict of interest.

References

1. Morimoto, R.I. The heat shock response: systems biology of proteotoxic stress in aging and disease. *Cold Spring Harb Symp Quant Biol* **2011**, *76*, 91-99.
2. Gomez-Pastor, R.; Burchfiel, E.T.; Thiele, D.J. Regulation of heat shock transcription factors and their roles in physiology and disease. *Nat Rev Mol Cell Biol* **2018**, *19*, 4-19.
3. Akerfelt, M.; Morimoto, R.I.; Sistonen, L. Heat shock factors: integrators of cell stress, development and lifespan. *Nat Rev Mol Cell Biol* **2010**, *11*, 545-555.
4. Murshid, A.; Eguchi, T.; Calderwood, S.K. Stress proteins in aging and life span. *Int J Hyperthermia* **2013**, *29*, 442-447.
5. Prince, T.L.; Lang, B.J.; Guerrero-Gimenez, M.E.; Fernandez-Munoz, J.M.; Ackerman, A.; Calderwood, S.K. HSF1: Primary Factor in Molecular Chaperone Expression and a Major Contributor to Cancer Morbidity. *Cells* **2020**, *9*.
6. Eguchi, T.; Sogawa, C.; Ono, K.; Matsumoto, M.; Tran, M.T.; Okusha, Y.; Lang, B.J.; Okamoto, K.; Calderwood, S.K. Cell Stress Induced Stressome Release Including Damaged Membrane Vesicles and Extracellular HSP90 by Prostate Cancer Cells. *Cells* **2020**, *9*, 755.
7. Ciocca, D.R.; Arrigo, A.P.; Calderwood, S.K. Heat shock proteins and heat shock factor 1 in carcinogenesis and tumor development: an update. *Arch Toxicol* **2013**, *87*, 19-48.
8. Eguchi, T.; Lang, B.J.; Murshid, A.; Prince, T.; Gong, J.; Calderwood, S.K. Regulatory roles for Hsp70 in cancer incidence and tumor progression. In *Frontiers in Structural Biology*, Galigniana, M.D., Ed. Bentham Science: 2018; Vol. 1, pp 1-22.
9. Chou, S.D.; Murshid, A.; Eguchi, T.; Gong, J.; Calderwood, S.K. HSF1 regulation of beta-catenin in mammary cancer cells through control of HuR/elavL1 expression. *Oncogene* **2015**, *34*, 2178-2188.
10. Gong, J.; Weng, D.; Eguchi, T.; Murshid, A.; Sherman, M.Y.; Song, B.; Calderwood, S.K. Targeting the hsp70 gene delays mammary tumor initiation and inhibits tumor cell metastasis. *Oncogene* **2015**, *34*, 5460-5471.
11. Trepel, J.; Mollapour, M.; Giaccone, G.; Neckers, L. Targeting the dynamic HSP90 complex in cancer. *Nat Rev Cancer* **2010**, *10*, 537-549.
12. Schopf, F.H.; Biebl, M.M.; Buchner, J. The HSP90 chaperone machinery. *Nat Rev Mol Cell Biol* **2017**, *18*, 345-360.
13. Tran, M.T.; Okusha, Y.; Feng, Y.; Sogawa, C.; Eguchi, T.; Kadowaki, T.; Sakai, E.; Tsukuba, T.; Okamoto, K. A novel role of HSP90 in regulating osteoclastogenesis by abrogating Rab11b-driven transport. *Biochim Biophys Acta Mol Cell Res* **2021**, *1868*, 119096.
14. Furuta, K.; Eguchi, T. Roles of Heat Shock Proteins on Antigen Presentation. In *Heat Shock Proteins in Human Diseases*, Asea, A.A.A.; Kaur, P., Eds. Springer Nature: Cham, Switzerland, 2020; Vol. 21, pp 275-280.
15. Lu, Y.; Eguchi, T.; Sogawa, C.; Taha, E.A.; Tran, M.T.; Nara, T.; Wei, P.; Fukuoka, S.; Miyawaki, T.; Okamoto, K. Exosome-Based Molecular Transfer Activity of Macrophage-Like Cells Involves Viability of Oral Carcinoma Cells: Size Exclusion Chromatography and Concentration Filter Method. *Cells* **2021**, *10*, 1328.
16. Saini, J.; Sharma, P.K. Clinical, Prognostic and Therapeutic Significance of Heat Shock Proteins in Cancer. *Curr Drug Targets* **2018**, *19*, 1478-1490.
17. Ono, K.; Eguchi, T.; Sogawa, C.; Calderwood, S.K.; Futagawa, J.; Kasai, T.; Seno, M.; Okamoto, K.; Sasaki, A.; Kozaki, K. HSP-enriched properties of extracellular vesicles involve survival of metastatic oral cancer cells. *J Cell Biochem* **2018**, *119*, 7350-7362.
18. Sasaya, T.; Kubo, T.; Murata, K.; Mizue, Y.; Sasaki, K.; Yanagawa, J.; Imagawa, M.; Kato, H.; Tsukahara, T.; Kanaseki, T., *et al.* Cisplatin-induced HSF1-HSP90 axis enhances the expression of functional PD-L1 in oral squamous cell carcinoma. *Cancer Med* **2022**.
19. Taha, E.A.; Ono, K.; Eguchi, T. Roles of Extracellular HSPs as Biomarkers in Immune Surveillance and Immune Evasion. *Int J Mol Sci* **2019**, *20*, 4588.
20. Ono, K.; Sogawa, C.; Kawai, H.; Tran, M.T.; Taha, E.A.; Lu, Y.; Oo, M.W.; Okusha, Y.; Okamura, H.; Ibaragi, S., *et al.* Triple knockdown of CDC37, HSP90-alpha and HSP90-beta diminishes extracellular vesicles-driven malignancy events and macrophage M2 polarization in oral cancer. *J Extracell Vesicles* **2020**, *9*, 1769373.
21. Eguchi, T.; Ono, K.; Kawata, K.; Okamoto, K.; Calderwood, S.K. Regulatory Roles of HSP90-Rich Extracellular Vesicles. In *Heat Shock Protein 90 in Human Diseases and Disorders*, Asea, A.A.A.; Kaur, P., Eds. Springer Nature: Cham, Swizerland, 2019; Vol. 19, pp 3-17.
22. Eguchi, T.; Sogawa, C.; Okusha, Y.; Uchibe, K.; Iinuma, R.; Ono, K.; Nakano, K.; Murakami, J.; Itoh, M.; Arai, K., *et al.* Organoids with Cancer Stem Cell-like Properties Secrete Exosomes and HSP90 in a 3D NanoEnvironment. *PLoS One* **2018**, *13*, e0191109.
23. Lu, Y.; Eguchi, T. HSP Stimulation on Macrophages Activates Innate Immune System. In *Heat Shock Proteins In Inflammatory Diseases*, Asea, A.A.A.; Punit, K., Eds. Springer Nature: Cham, Switzerland, 2021; Vol. 22, pp 53-68.
24. Sheta, M.; Taha, E.A.; Lu, Y.; Eguchi, T. Extracellular Vesicles: New Classification and Tumor Immunosuppression. *Biology* **2023**, *12*.

25. Anckar, J.; Sistonen, L. Regulation of HSF1 function in the heat stress response: implications in aging and disease. *Annu Rev Biochem* **2011**, *80*, 1089-1115.
26. Mendillo, M.L.; Santagata, S.; Koeva, M.; Bell, G.W.; Hu, R.; Tamimi, R.M.; Fraenkel, E.; Ince, T.A.; Whitesell, L.; Lindquist, S. HSF1 drives a transcriptional program distinct from heat shock to support highly malignant human cancers. *Cell* **2012**, *150*, 549-562.
27. Chou, S.D.; Prince, T.; Gong, J.; Calderwood, S.K. mTOR is essential for the proteotoxic stress response, HSF1 activation and heat shock protein synthesis. *PLoS One* **2012**, *7*, e39679.
28. Eguchi, T.; Calderwood, S.K.; Takigawa, M.; Kubota, S.; Kozaki, K. Intracellular MMP3 Promotes HSP Gene Expression in Collaboration With Chromobox Proteins. *J Cell Biochem* **2017**, *118*, 43-51.
29. Tadepally, H.D.; Burger, G.; Aubry, M. Evolution of C2H2-zinc finger genes and subfamilies in mammals: species-specific duplication and loss of clusters, genes and effector domains. *BMC Evol Biol* **2008**, *8*, 176.
30. Edelstein, L.C.; Collins, T. The SCAN domain family of zinc finger transcription factors. *Gene* **2005**, *359*, 1-17.
31. Sander, T.L.; Stringer, K.F.; Maki, J.L.; Szauter, P.; Stone, J.R.; Collins, T. The SCAN domain defines a large family of zinc finger transcription factors. *Gene* **2003**, *310*, 29-38.
32. Schumacher, C.; Wang, H.; Honer, C.; Ding, W.; Koehn, J.; Lawrence, Q.; Coulis, C.M.; Wang, L.L.; Ballinger, D.; Bowen, B.R., *et al.* The SCAN domain mediates selective oligomerization. *J Biol Chem* **2000**, *275*, 17173-17179.
33. Williams, A.J.; Blacklow, S.C.; Collins, T. The zinc finger-associated SCAN box is a conserved oligomerization domain. *Mol Cell Biol* **1999**, *19*, 8526-8535.
34. Eguchi, T.; Prince, T.; Wegiel, B.; Calderwood, S.K. Role and Regulation of Myeloid Zinc Finger Protein 1 in Cancer. *J Cell Biochem* **2015**, *116*, 2146-2154.
35. Sander, T.L.; Haas, A.L.; Peterson, M.J.; Morris, J.F. Identification of a novel SCAN box-related protein that interacts with MZF1B. The leucine-rich SCAN box mediates hetero- and homoprotein associations. *J Biol Chem* **2000**, *275*, 12857-12867.
36. Perrotti, D.; Melotti, P.; Skorski, T.; Casella, I.; Peschle, C.; Calabretta, B. Overexpression of the zinc finger protein MZF1 inhibits hematopoietic development from embryonic stem cells: correlation with negative regulation of CD34 and c-myb promoter activity. *Mol Cell Biol* **1995**, *15*, 6075-6087.
37. Eguchi, T.; Prince, T.L.; Tran, M.T.; Sogawa, C.; Lang, B.J.; Calderwood, S.K. MZF1 and SCAND1 Reciprocally Regulate CDC37 Gene Expression in Prostate Cancer. *Cancers (Basel)* **2019**, *11*, 792.
38. Zheng, L.; Jiao, W.; Mei, H.; Song, H.; Li, D.; Xiang, X.; Chen, Y.; Yang, F.; Li, H.; Huang, K., *et al.* miRNA-337-3p inhibits gastric cancer progression through repressing myeloid zinc finger 1-facilitated expression of matrix metalloproteinase 14. *Oncotarget* **2016**, *7*, 40314-40328.
39. Ko, H.; Kim, S.; Yang, K.; Kim, K. Phosphorylation-dependent stabilization of MZF1 upregulates N-cadherin expression during protein kinase CK2-mediated epithelial-mesenchymal transition. *Oncogenesis* **2018**, *7*, 27.
40. Luan, H.; Mohapatra, B.; Bielecki, T.A.; Mushtaq, I.; Mirza, S.; Jennings, T.A.; Clubb, R.J.; An, W.; Ahmed, D.; El-Ansari, R., *et al.* Loss of the Nuclear Pool of Ubiquitin Ligase CHIP/STUB1 in Breast Cancer Unleashes the MZF1-Cathepsin Pro-oncogenic Program. *Cancer Res* **2018**, *78*, 2524-2535.
41. Verma, N.K.; Gadi, A.; Maurizi, G.; Roy, U.B.; Mansukhani, A.; Basilico, C. Myeloid Zinc Finger 1 and GA Binding Protein Co-Operate with Sox2 in Regulating the Expression of Yes-Associated Protein 1 in Cancer Cells. *Stem Cells* **2017**, *35*, 2340-2350.
42. Wu, L.; Han, L.; Zhou, C.; Wei, W.; Chen, X.; Yi, H.; Wu, X.; Bai, X.; Guo, S.; Yu, Y., *et al.* TGF-beta1-induced CK17 enhances cancer stem cell-like properties rather than EMT in promoting cervical cancer metastasis via the ERK1/2-MZF1 signaling pathway. *FEBS J* **2017**, *284*, 3000-3017.
43. Eguchi, T.; Csizmadia, E.; Kawai, H.; Sheta, M.; Yoshida, K.; Prince, T.L.; Wegiel, B.; Calderwood, S.K. SCAND1 Reverses Epithelial-to-Mesenchymal Transition (EMT) and Suppresses Prostate Cancer Growth and Migration. *Cells* **2022**, *11*.
44. Tsai, S.J.; Hwang, J.M.; Hsieh, S.C.; Ying, T.H.; Hsieh, Y.H. Overexpression of myeloid zinc finger 1 suppresses matrix metalloproteinase-2 expression and reduces invasiveness of SiHa human cervical cancer cells. *Biochem Biophys Res Commun* **2012**, *425*, 462-467.
45. Wu, D.; Tan, H.; Su, W.; Cheng, D.; Wang, G.; Wang, J.; Ma, D.A.; Dong, G.M.; Sun, P. MZF1 mediates oncogene-induced senescence by promoting the transcription of p16(INK4A). *Oncogene* **2022**, *41*, 414-426.
46. Noll, L.; Peterson, F.C.; Hayes, P.L.; Volkman, B.F.; Sander, T. Heterodimer formation of the myeloid zinc finger 1 SCAN domain and association with promyelocytic leukemia nuclear bodies. *Leuk Res* **2008**, *32*, 1582-1592.
47. Dupuy, D.; Aubert, I.; Dupérat, V.G.; Petit, J.; Taine, L.; Stef, M.; Bloch, B.; Arveiler, B. Mapping, characterization, and expression analysis of the SM-20 human homologue, c1orf12, and identification of a novel related gene, SCAND2. *Genomics* **2000**, *69*, 348-354.

48. Nakai, A.; Tanabe, M.; Kawazoe, Y.; Inazawa, J.; Morimoto, R.I.; Nagata, K. HSF4, a new member of the human heat shock factor family which lacks properties of a transcriptional activator. *Mol Cell Biol* **1997**, *17*, 469-481.
49. Zhang, W.; Zhang, X.; Cheng, P.; Yue, K.; Tang, M.; Li, Y.; Guo, Q.; Zhang, Y. HSF4 promotes tumor progression of colorectal cancer by transactivating c-MET. *Mol Cell Biochem* **2022**.
50. Ma, P.; Tang, W.G.; Hu, J.W.; Hao, Y.; Xiong, L.K.; Wang, M.M.; Liu, H.; Bo, W.H.; Yu, K.H. HSP4 triggers epithelial-mesenchymal transition and promotes motility capacities of hepatocellular carcinoma cells via activating AKT. *Liver Int* **2020**, *40*, 1211-1223.
51. Jin, X.; Eroglu, B.; Cho, W.; Yamaguchi, Y.; Moskophidis, D.; Mivechi, N.F. Inactivation of heat shock factor Hsf4 induces cellular senescence and suppresses tumorigenesis in vivo. *Mol Cancer Res* **2012**, *10*, 523-534.
52. Eguchi, T.; Sheta, M.; Fujii, M.; Calderwood, S.K. Cancer Extracellular Vesicles, Tumoroid Models, and Tumor Microenvironment. *Semin Cancer Biol* **2022**, *86*, 112-126.
53. Namba, Y.; Sogawa, C.; Okusha, Y.; Kawai, H.; Itagaki, M.; Ono, K.; Murakami, J.; Aoyama, E.; Ohyama, K.; Asaumi, J., *et al.* Depletion of Lipid Efflux Pump ABCG1 Triggers the Intracellular Accumulation of Extracellular Vesicles and Reduces Aggregation and Tumorigenesis of Metastatic Cancer Cells. *Front Oncol* **2018**, *8*, 1-16.
54. Yoshida, S.; Kawai, H.; Eguchi, T.; Sukegawa, S.; Oo, M.W.; Anqi, C.; Takabatake, K.; Nakano, K.; Okamoto, K.; Nagatsuka, H. Tumor Angiogenic Inhibition Triggered Necrosis (TAITN) in Oral Cancer. *Cells* **2019**, *8*, 761.
55. Gilkes, D.M.; Semenza, G.L.; Wirtz, D. Hypoxia and the extracellular matrix: drivers of tumour metastasis. *Nat Rev Cancer* **2014**, *14*, 430-439.
56. Boedtkjer, E.; Pedersen, S.F. The Acidic Tumor Microenvironment as a Driver of Cancer. *Annu Rev Physiol* **2020**, *82*, 103-126.
57. Fais, S.; Venturi, G.; Gatenby, B. Microenvironmental acidosis in carcinogenesis and metastases: new strategies in prevention and therapy. *Cancer Metastasis Rev* **2014**, *33*, 1095-1108.
58. Ischia, J.; So, A.I. The role of heat shock proteins in bladder cancer. *Nat Rev Urol* **2013**, *10*, 386-395.
59. Torigoe, T.; Tamura, Y.; Sato, N. Heat shock proteins and immunity: application of hyperthermia for immunomodulation. *Int J Hyperthermia* **2009**, *25*, 610-616.
60. Wiersma, V.R.; Michalak, M.; Abdullah, T.M.; Bremer, E.; Eggleton, P. Mechanisms of Translocation of ER Chaperones to the Cell Surface and Immunomodulatory Roles in Cancer and Autoimmunity. *Front Oncol* **2015**, *5*, 7.
61. Kamikawa, Y.; Saito, A.; Imaizumi, K. Impact of Nuclear Envelope Stress on Physiological and Pathological Processes in Central Nervous System. *Neurochem Res* **2022**, *47*, 2478-2487.
62. Panagaki, D.; Croft, J.T.; Keuenhof, K.; Larsson Berglund, L.; Andersson, S.; Kohler, V.; Buttner, S.; Tamas, M.J.; Nystrom, T.; Neutze, R., *et al.* Nuclear envelope budding is a response to cellular stress. *Proc Natl Acad Sci U S A* **2021**, *118*.
63. Xu, B.; Sun, Z.; Liu, Z.; Guo, H.; Liu, Q.; Jiang, H.; Zou, Y.; Gong, Y.; Tischfield, J.A.; Shao, C. Replication stress induces micronuclei comprising of aggregated DNA double-strand breaks. *PLoS One* **2011**, *6*, e18618.
64. Ahn, S.G.; Thiele, D.J. Redox regulation of mammalian heat shock factor 1 is essential for Hsp gene activation and protection from stress. *Genes Dev* **2003**, *17*, 516-528.
65. Gong, J.L.; Lang, B.J.; Weng, D.S.; Eguchi, T.; Murshid, A.; Borges, T.J.; Doshi, S.; Song, B.Z.; Stevenson, M.A.; Calderwood, S.K. Genotoxic stress induces Sca-1-expressing metastatic mammary cancer cells. *Molecular Oncology* **2018**, *12*, 1249-1263.
66. Hitomi, K.; Okada, R.; Loo, T.M.; Miyata, K.; Nakamura, A.J.; Takahashi, A. DNA Damage Regulates Senescence-Associated Extracellular Vesicle Release via the Ceramide Pathway to Prevent Excessive Inflammatory Responses. *Int J Mol Sci* **2020**, *21*.
67. Guang, M.H.Z.; Kavanagh, E.L.; Dunne, L.P.; Dowling, P.; Zhang, L.; Lindsay, S.; Bazou, D.; Goh, C.Y.; Hanley, C.; Bianchi, G., *et al.* Targeting Proteotoxic Stress in Cancer: A Review of the Role that Protein Quality Control Pathways Play in Oncogenesis. *Cancers (Basel)* **2019**, *11*.
68. Dreos, R.; Ambrosini, G.; Groux, R.; Cavin Perier, R.; Bucher, P. The eukaryotic promoter database in its 30th year: focus on non-vertebrate organisms. *Nucleic Acids Res* **2017**, *45*, D51-d55.
69. Taha, E.A.; Sogawa, C.; Okusha, Y.; Kawai, H.; Oo, M.W.; Elseoudi, A.; Lu, Y.; Nagatsuka, H.; Kubota, S.; Satoh, A., *et al.* Knockout of MMP3 Weakens Solid Tumor Organoids and Cancer Extracellular Vesicles. *Cancers (Basel)* **2020**, *12*, 1260.
70. Okusha, Y.; Eguchi, T.; Tran, M.T.; Sogawa, C.; Yoshida, K.; Itagaki, M.; Taha, E.A.; Ono, K.; Aoyama, E.; Okamura, H., *et al.* Extracellular Vesicles Enriched with Moonlighting Metalloproteinase Are Highly Transmissive, Pro-Tumorigenic, and Trans-Activates Cellular Communication Network Factor (CCN2/CTGF): CRISPR against Cancer. *Cancers (Basel)* **2020**, *12*, 881.
71. Vargas, J.N.S.; Hamasaki, M.; Kawabata, T.; Youle, R.J.; Yoshimori, T. The mechanisms and roles of selective autophagy in mammals. *Nat Rev Mol Cell Biol* **2022**.

72. Gao, J.; Aksoy, B.A.; Dogrusoz, U.; Dresdner, G.; Gross, B.; Sumer, S.O.; Sun, Y.; Jacobsen, A.; Sinha, R.; Larsson, E., *et al.* Integrative analysis of complex cancer genomics and clinical profiles using the cBioPortal. *Sci Signal* **2013**, *6*, pl1.
73. Li, C.; Tang, Z.; Zhang, W.; Ye, Z.; Liu, F. GEPIA2021: integrating multiple deconvolution-based analysis into GEPIA. *Nucleic Acids Res* **2021**, *49*, W242-w246.
74. Lánczky, A.; Győrffy, B. Web-Based Survival Analysis Tool Tailored for Medical Research (KMplot): Development and Implementation. *J Med Internet Res* **2021**, *23*, e27633.